Published Online First: June, 2024
https://doi.org/10.21123/bsj.2024.9322
P-ISSN: 2078-8665 - E-ISSN: 2411-7986
Baghdad Science Journal

# Comparative analysis of plasma generated using LIBS technique for different wavelengths of pulsed laser of a cadmium target

***Tuqa A. Khalepha*, *Nisreen Kh. Abdalameer***

Department of Physics, College of Science for Women, University of Baghdad, Baghdad, Iraq.
*Corresponding Author.

Received 09/09/2023, Revised 23/02/2024, Accepted 25/02/2024, Published Online First 20/06/2024



## Abstract

The objective of this study is to analyze the spectral properties of plasma produced from cadmium (Cd) by utilizing the Laser-Induced Breakdown Spectroscopy (LIBS) method. The plasma generation process employed the primary (1064 nm) fundamental harmonic laser (FHL) and the secondary (532 nm) second harmonic laser (SHL) of a Q-switched neodymium-doped laser. Yttrium aluminum Garnet (YAG) is used as a crystalline substance. The laser pulses have a duration of 10 ns, and a repetition rate of 8 Hz and the energy outputs were 250 (mJ) and 500 (mJ) at wavelengths of 1064 (nm) and 532 (nm), respectively. The achievement of precise beam focus was accomplished by focusing the laser onto the target material, which consisted of 100% cadmium. The electron temperature was measured using the Boltzmann plot approach by harnessing empirical data on linear properties associated with neutral lines (Cd II), (O II), (N II), and ion lines (Cd I), (O I) for (1064, 532) nm. The use of an analytical methodology resulted in the determination of electron temperature values of 8584 K to 15068.4 K for the fundamental and second harmonics of the laser, respectively. Simultaneously, the electron density ($n_e$) was determined by analyzing the Stark broadening profile linked to the neutral cadmium line. The plasma characteristics (electron temperature and electron density) are determined by the modulation of laser energy at the surface of the target, longitudinally along the trajectory of the plasma plume.

**Keywords:** Boltzmann plot methodology, electron temperature, electron density, LIBS, SHG, Stark broadening.

## Introduction

Laser-induced breakdown spectroscopy (LIBS) is a very adaptable method used for the examination and quantification of various substances. It relies on the optical identification of specific atomic and molecular components by observing the emission signals emitted from plasma generated by laser-induced processes [1]. The approach under consideration is characterized by its relative simplicity in comparison to many other elemental analysis methods. This attribute may be attributed to its uncomplicated experimental setup. The experimental setup involves the use of a pulsed laser to induce microplasma formation on the surface of interest [2]. Subsequently, the elemental composition is determined by analyzing the emitted radiation from the plasma plume [3]. The characteristics and behavior of laser-induced plasma are influenced by multiple parameters, including the wavelength of the laser, the dimensions of the laser spot, and the temporal length of the laser pulse. The surrounding

Published Online First: June, 2024
https://doi.org/10.21123/bsj.2024.9322
P-ISSN: 2078-8665 - E-ISSN: 2411-7986
Baghdad Science Journal

environment and other relevant parameters. Experiments may be conducted under two conditions: atmospheric pressure or in the presence of an ambient gas, using this particular approach [4]. The ablation process entails the use of laser energy to disperse throughout the sample via heat conduction, leading to the fusion and vaporization of the target material. As a result, a plasma plume is generated. One significant advantage of using this technology is its capacity to provide a direct chemical analysis of the substance without requiring any further preparation [5]. The ablation method, which involves the use of lasers with pulse lengths exceeding [6] nanoseconds, may be divided into three separate phases. In the first phase, the laser beam engages with the solid material, resulting in the fast ionization of the target's surface. The ionization process takes place within a temporal duration that is less than the temporal extent of the laser pulse [7]. In the subsequent phase, the plasma, leading to an isothermal expansion, efficiently absorbs the laser. During the third stage, after the cessation of the laser pulse, the plasma plume that emerges experiences a quasi-adiabatic expansion inside a medium [8]. The medium under consideration may include either a state of vacuum or a background gas, and its composition may or may not involve the existence of externally imposed fields [9]. Passive optical emission spectroscopy (OES) is a prominent diagnostic tool used in plasma characterization [10]. OES is a cost-effective, versatile, and unobtrusive technique for investigating plasmas with low temperatures and pressures[11]. It has exhibited adaptability in determining the density of electrons and the temperature of these discharges. To perform OES, it is essential to have a spectrometer with the suitable resolution and optical equipment that can effectively transport emitted light to the entry slit of the spectrometer[12]. While it is easy to acquire emission spectra, interpreting them may be somewhat intricate, especially in low-temperature, low-pressure plasmas [13] that are far from thermal equilibrium. The processing parameters, such as the power and flow rate of the working gas, have significant effects on obtaining the desired performance in low-temperature plasma processes, such as etching, sputtering, and deposition [14, 15]. In this study, an investigation into the emission characteristics of plasma produced on the surface of cadmium by the use of an Nd: YAG laser is presented. The transitions observed in this work include the wavelengths of 247.85 nm, 394.22 nm, 396.14 nm, 588.95 nm, and 591.25 nm in neutral cadmium. These transitions were investigated to analyze the spatial characteristics by calculating the plasma parameters. Furthermore, different laser energy levels and wavelengths are used to investigate the temperature and electron density of the ablated plasma plume of Cd.

## Materials and Methods

### Preparation the Sample

The focus of this experimental investigation was the analysis of a sample consisting solely of cadmium (Cd), with a mass percentage of 100%. A hydraulic press machine was employed to create a pellet measuring 10 mm in diameter and 4 mm in thickness, with a load of 10 tons for 15 minutes. The pellet was formed from a small quantity of material.

### Experimental Setup

The experimental configuration is shown in Fig. 1. Experiments have been done under standard ambient conditions, namely at room temperature and atmospheric pressure. The plasma is generated by using pulses emitted from the Nd: YAG nanosecond laser, namely the 1064 FHG and 532 SHG wavelengths. These pulses possess an energy of 250, and 500 mJ, a pulse duration of 10 ns, and a repetition frequency of 8 Hz. The subject of interest in this study was cadmium, which exhibited a high level of purity, with a concentration of around 99.999%. The laser beam is directed onto the surface of a cadmium pallet that is present in the air at atmospheric pressure. This is achieved by using a quartz lens with a focal length of 10 cm. The optical emission light was acquired and examined using a Surwit (S3000-UV-NIR) spectrometer, using an optic fiber bundle with a core diameter of 50 µm. The fiber was positioned at a distance of 1 cm. The plasma properties were estimated by using the NIST database software [16] to measure the optical emission

Published Online First: June, 2024
https://doi.org/10.21123/bsj.2024.9322
P-ISSN: 2078-8665 - E-ISSN: 2411-7986
Baghdad Science Journal

line outcomes of certain components as show in Tables 1 and Table 2.

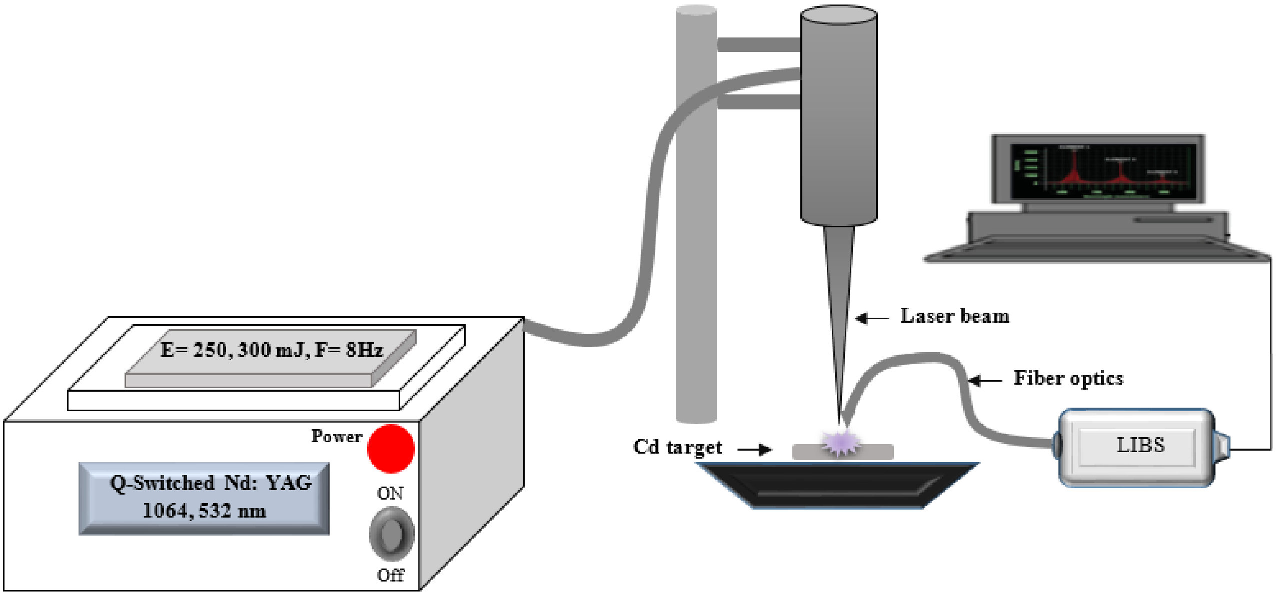


**Figure 1. Block diagram of the experimental setup of the LIBS system**

**Table 1. Parameters of the spectroscopy of measured linens emitted from Cd plasma plume corresponding to the NIST database by first harmonic generation laser [16]**

| λ = 1064 nm | | | | | |
|---|---|---|---|---|---|
| **Spectral Lines** | **Wavelength (nm)** | **Lower Level** | **Upper Level** | $A_k.g_k$ | $E_k$ **(eV)** |
| Cd II | 428.5 | $4d^{10}6p$ | $4d^{10}7d$ | 2.4 E+07 | 11.8 |
| Cd II | 444.05 | $4d^{10}4f$ | $4d^{10}9g$ | 7.66 E+06 | 13.44 |
| Cd I | 467.8 | $4d^{10}5s5p$ | $4d^{10}5s6d$ | 2.8 E+07 | 5.41 |
| Cd II | 474.46 | $4d^{10}4f$ | $4d^{10}8g$ | 3.9 E+07 | 13.7 |
| Cd II | 502.8 | $4d^{10}5d$ | $4d^{9}5s(^{3}D)5p$ | 1.91 E+08 | 11.13 |
| Cd I | 508.58 | $4d^{10}5s5p$ | $4d^{10}5s6s$ | 1.7 E+08 | 5.41 |
| Cd I | 515 | $4d^{10}5s5p$ | $4d^{10}5s7s$ | 1.7 E+08 | 5.41 |
| Cd II | 538.18 | $4d^{10}5d$ | $4d^{10}4f$ | 7.26 E+07 | 11.13 |
| O I | 556.98 | $2s^{2}2p^{3}(^{4}S^{0})3P$ | $2s^{2}2p^{3}(^{4}S^{0})7S$ | 5.82E+05 | 13.22 |
| N II | 563.48 | $2s^{2}2p4P$ | $2s^{2}2p6s$ | 3.54E+07 | 27.66 |
| Cd I | 632.51 | $4d^{10}5s5p$ | $4d^{10}5s5d$ | 7.26 E+07 | 5.41 |
| Cd II | 635.99 | $4d^{10}4f$ | $4d^{10}6g$ | 7.26 E+07 | 13.44 |

**Table 2. Parameters of the spectroscopy of measured linens emitted from Cd plasma plume corresponding to the NIST database by second harmonic generation laser [16]**

| λ = 532 nm | | | | | |
|---|---|---|---|---|---|
| **Spectral Lines** | **Wavelength (nm)** | **Lower Level** | **Upper Level** | $A_k.g_k$ | $E_k$ **(eV)** |
| Cd I | 467.8 | $4d^{10}5s5p$ | $4d^{10}5s6d$ | 2.8 E+07 | 5.41 |
| Cd II | 502.8 | $4d^{10}5d$ | $4d^{9}5s(^{3}D)5p$ | 1.91 E+08 | 11.13 |
| Cd II | 538.18 | $4d^{10}5d$ | $4d^{10}4f$ | 7.26 E+07 | 11.13 |
| O II | 548.34 | $2s^{2}2p^{2}(^{3}P)3p$ | $2s^{2}2p^{2}(^{3}P)3d$ $4d$ | 5.04 E+07 | 71.39 |
| Cd II | 584.33 | $4d^{10}6d$ | $^{10}7f$ | 7.26 E+07 | 13.65 |
| Cd II | 656.33 | $4d^{10}7p$ | $4d^{10}9d$ | 7.26 E+07 | 13.65 |

Published Online First: June, 2024
https://doi.org/10.21123/bsj.2024.9322
P-ISSN: 2078-8665 - E-ISSN: 2411-7986
Baghdad Science Journal

## Results and Discussion

The breakdown encompasses a range of events, including surface sample heating accompanied by phase change and photoelectric emissions, as well as the presence of thermal ions and neutral plasma molecules. The evolution of laser-induced plasma encompasses a series of sequential processes. Initially, the emission of steady bremsstrahlung radiation takes place, followed by the subsequent expansion and cooling of the plasma. The detection of emissions of spectral lines occurring between closely linked energy levels is possible during the subsequent relaxation of the plasma. Following the production of plasma, these lines are observed to be embedded within a stream of continuous emissions. Hence, the phenomenon of complete plasma radiation is initially observed as a continuous spectrum and comprises electronically excited pieces that undergo spontaneous decay, namely ions, atoms, and tiny molecules [17]. The plasma emissions were collected and subjected to analysis using an optical fiber bundle, which was then combined with a spectrometer. The spectrum peak intensities of the Cd plasma plume, caused by an Nd: YAG nanosecond laser, are depicted in Figs. 2-a and 2-b. The laser was operated with energies of 250, and 500 mJ and emitted at two different wavelengths: the first harmonic at 1064 nm and the second harmonic at 532 nm. The relationship between laser energy and the observed intensity and width of spectral lines has been noted to be positive, indicating that as laser energy increases, both the intensity and width of the spectral lines also rise.

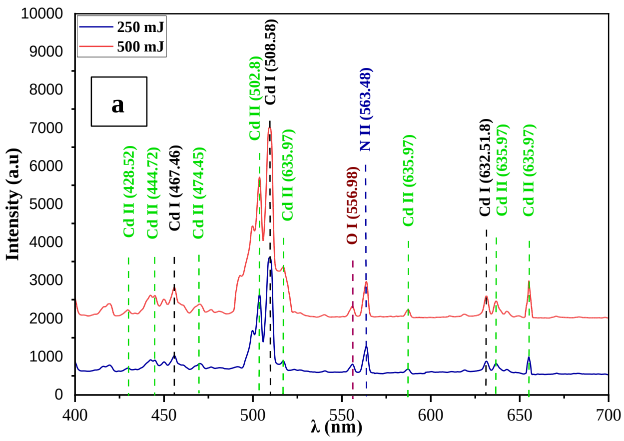


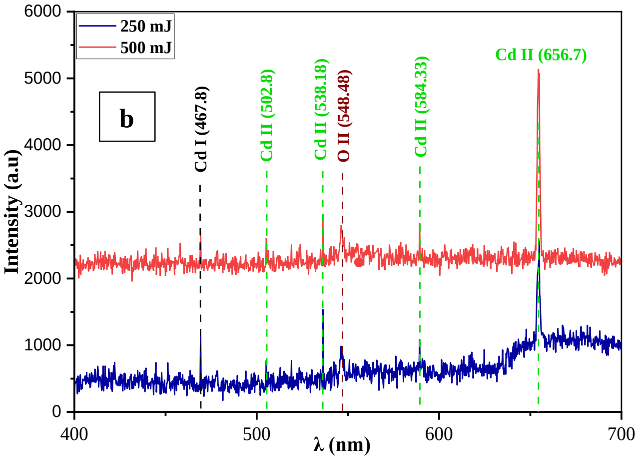


**Figure 2. Displays the emission spectra of Cadmium plasma inside a distinct window, encompassing the spectral ranges of 400 to 700 nm. These spectra are generated by the utilization of the (a) first harmonic 1064 nm and (b) second harmonic 532 nm of the laser for different laser energy.**

The spectrum covers the 400 to 700 nm spectral region by the induced fundaments laser; most lines in the spectral region contain neutral Cadmium emissions and the strongest spectral line of Cd I and OI at 467.8, 508.58, 515, and 632.51 nm while 556.98 nm to OI are specified as $4d^{10}5s5p \rightarrow 4d^{10}5s6d$, $4d^{10}5s5p \rightarrow 4d^{10}5s6s$, $4d^{10}5s5p \rightarrow 4d^{10}5s7s$, and $4d^{10}5s5p \rightarrow 4d^{10}5s5d$, while $2s^22p3\ (4S^0)3P \rightarrow 2s^22p3\ (4S^0)7S$ transitions, respectively. And spectral region ranging between 400-650 nm is dominated by ionic lines (Cd II) and (N II), the most robust spectral lines at 502.8 and 635.97 nm for Cd but N at 563.48 nm are specified as $4d^{10}5d \rightarrow 4d^95s(3D)5p$ and $4d^{10}4f \rightarrow 4d^{10}6g$ for Cd but $2s^22p4P \rightarrow 2s^22p6s$ for N transitions, respectively. While in a second laser, the spectral emitting region ranging from 400 to 700 nm is covered by the plasma spectrum that is emitted by the induced second harmonic laser (532 nm), the spectral emitting region at 467 nm is ascribed to neutral Cadmium line (Cd I); the line is specified for 467.8 nm as $4d^{10}5s5p \rightarrow 4d^{10}5s6d$, transitions, and spectral region ranged between 500-700 nm is dominated by ionic lines (Cd II), the most robust spectral lines at 538.18 and 656.7 nm are specified as $4d^{10}5d \rightarrow 4d^{10}4f$ and $4d^{10}7p \rightarrow 4d^{10}9d$ transitions, respectively [16].

Published Online First: June, 2024
https://doi.org/10.21123/bsj.2024.9322
P-ISSN: 2078-8665 - E-ISSN: 2411-7986
Baghdad Science Journal

## Calculate plasma parameters and LTE criterion

### Plasma temperature

Studies of laser-induced plasma emitted spectra help estimate the essential plasma parameters (i.e., Te and ne). In addition, the concept of the plasma characteristics depended on the electron temperature and described the relative distribution of the population by the Boltzmann law of the atoms over their energy level [6]. The Boltzmann plot method determined the plasma electron temperature based on the intensity of the observed spectral line. The plasma temperature equation can be written as in Eq. 1 [18] due to the predicted local thermodynamic equilibrium:

$$\mathrm{Ln}\left(\frac{I_{ji}\lambda_{ji}}{A_{ji}g_{ji}}\right) = \frac{E_j}{k_B T_e} + C \;\; \dots\dots\dots 1$$

Here, line identification and various spectroscopic parameters, including wavelength ($j_i$), statistical weight ($g$), probability of transition ($A_{ji}$), and upper energy ($E$), obtained from a standard spectrum of the *NIST* database [16] and listed in Table 1, $i$ and $j$ refer to the low and upper levels, respectively. ($k_B$) is the Boltzmann constant, $T$ is the plasma temperature, and $C$ is the constant. To draw the Boltzmann plot, we used the atomic Cadimuim Cd (I) lines to deduce the plasma electron temperature, as shown in Fig. 3 of 1064 nm and Fig. 4 of 532 nm laser. The temperature of the electron can be estimated from the slope obtained from a graph $Ln\left(\frac{I_{ji}\lambda_{ji}}{A_{ji}g_{ji}}\right)$ versus the energy $E_j$ (eV) a straight line has an equal slope $\frac{1}{k_B T_e}$

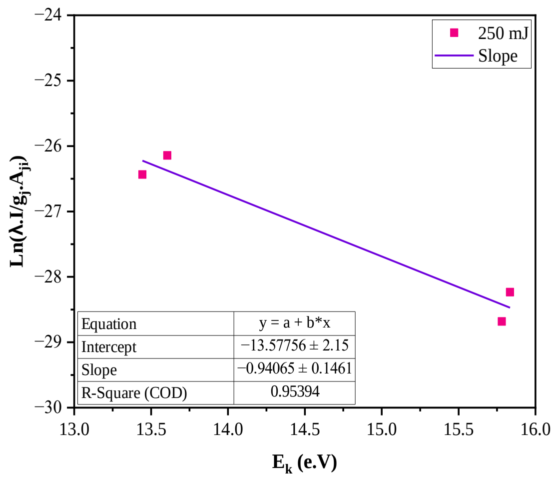


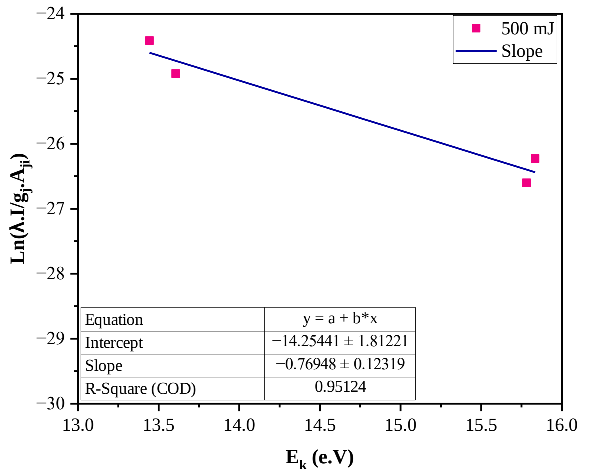


**Figure 3. Boltzmann plot for 4 neutral and ion c spectral lines at laser energy 250-500 mJ using λ 1064 mm.**

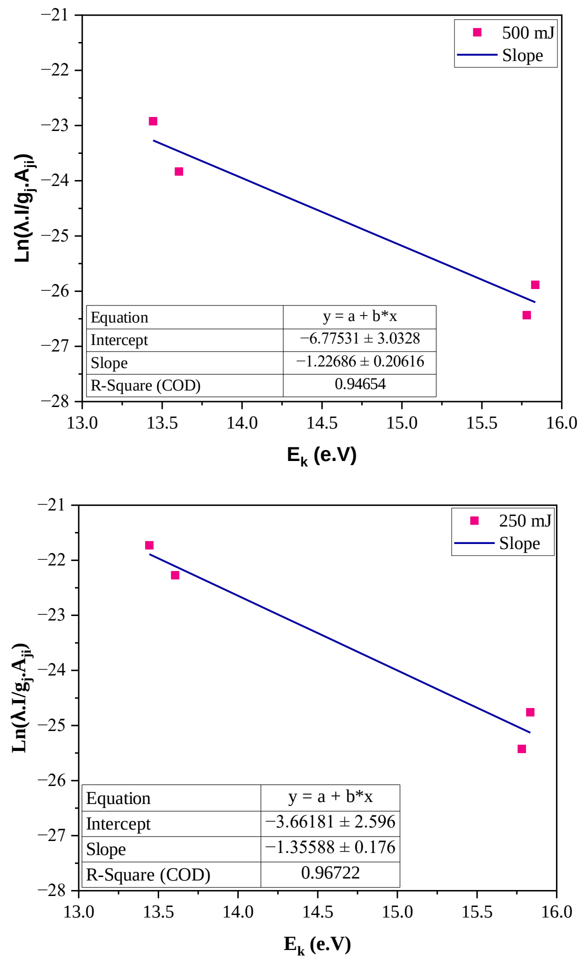


**Figure 4. Boltzmann plot for 4 neutral and ion c spectral lines at laser energy range 250-500 mJ using λ 532 mm**

Published Online First: June, 2024
https://doi.org/10.21123/bsj.2024.9322
P-ISSN: 2078-8665 - E-ISSN: 2411-7986
Baghdad Science Journal

The electron temperature in Cd plasma plumes was calculated by changing the pulse laser energy to 250, and 500 mJ at both modes (1064 and 532 nm) of the Nd: YAG laser. Depending on laser pulse energy and wavelength, Cd plasma plumes' temperature values range from 8540 to 15068 K, as seen in Tables 3, and 4. The electron temperature is higher as the laser energy and wavelength increase and ranges from 12330.8 to 15068.4 K for the plasma caused by the λ 1064 nm. However, we noticed that the electron temperature ranged from 8540 to 9512 K when repeating the experiment using the λ 532 mm at the same ambient conditions.

Fig. 5, also indicates that electron temperature behavior increases with the wavelength. The increased transfer of laser-plasma energy likely causes increased laser pulse energy and wavelength which elevates the plasma temperature which is in agreement with the previous studies [15]. The electron temperatures exhibit a positive correlation with the energy of the plasma plume laser, primarily influenced by the phenomena of plasma reflection and absorption of laser photons, contingent upon the plasma frequency [19]. The Cadmium plasma frequency appears to be lower than that of the laser. It means that energy loss is due to the neglected Nd: YAG laser reflection on the Cd plasma surface [20].

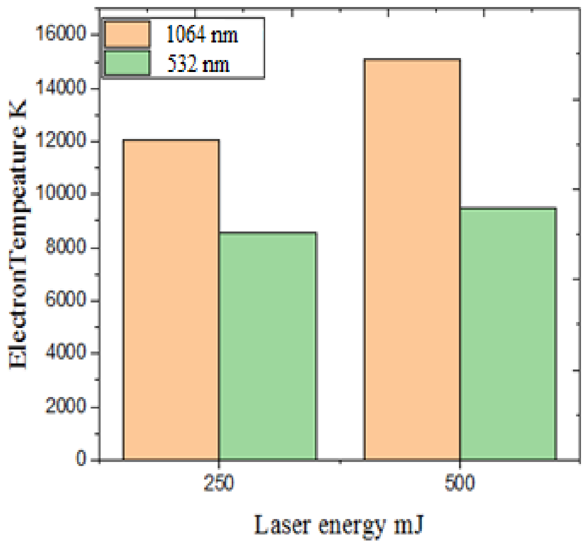


**Figure 5. The electron temperature at λ 1064 and 532 nm as a function of laser energy**

It is possible to understand two reasons why the plasma plume's temperature increases with the laser pulse's energy. First, the result of an increase in the rate of mass ablation [21]. Second, one of the two possibilities of interaction is called "plasma shielding"[22]. The first reason is when the plasma is created, through electron-neutral inverse-Bremsstrahlung or electron-ion inverse-Bremsstrahlung, the plasma will absorb part of the laser beam, and the second reason is through the photo-ionization dominated interaction. Except for the early phases of the laser evaporation process, the electron-neutral process's probability is much less than that of the electron-ion processes. Thus, electron-neutral processes during laser ablation are considered negligible [23].

**Electron Density**

The electron number density is a significant parameter used to describe the plasma environment, which is essential for evaluating its equilibrium (LTE) criterion. The Stark broadening line profile of an isolated single charged ion or line neutral is one of the main methods used for estimating the electron number density ($n_e$.). Stark broadening is one of the dominant broadening methods in LIP, with 2- 4 orders larger than other methods such as natural broadening and Doppler broadening [24]. The plasma ne electron density is indicated by Eq. 2 for the full width at half maximum (FWHM) of the Stark broadening lines [25]:

$$\Delta\lambda_{\frac{1}{2}} = 2\omega\left(\frac{n_e}{10^{16}}\right) + 3.5\,A\left(\frac{n_e}{10^{16}}\right)^{\frac{5}{4}}\left[1 - \frac{3}{4}N_D^{-1/3}\right]\omega \ldots\ldots\ldots 2$$

In empirical formula (2), $\Delta\lambda_{\frac{1}{2}}$ refers to the Stark full-width at half-maximum (FHWM), and $\omega$ is the electron impact parameter, which is based on reference data, which corresponds to different electron temperatures. $n_e$, $A\ nm$, and $N_D$ denotes the electron density, broadening ionic impact parameter, and the number of particles in the Debye sphere. The ionic broadening was neglected due to its minimal [26] contribution to the broadening: hence Eq. 2. can then be defined in Eq. 3. The electron density $n_e$ corresponds to the (FWHM) of the Stark broadening lines of the plasma plume [27]:

Published Online First: June, 2024
https://doi.org/10.21123/bsj.2024.9322
P-ISSN: 2078-8665 - E-ISSN: 2411-7986
Baghdad Science Journal

$$n_e = \left(\frac{\Delta\lambda}{2w_s}\right) N_r \ldots \ldots \ldots 3$$

Figs. 6-a and 6-b illustrate the full width at half maximum (FWHM) of the Stark-broadened profile of the N II, and Cd II emission lines for FHG and SHG respectively, which may be used to calculate the Stark broadening center of 563.48, and 656.33 nm respectively. In comparison to the practical and theoretical values that were given in the literature, $w_s$ (0.204, and 0.04) A° were utilized at a $N_r$ equal to (0.99 x $10^{17}$, and 1.00 x $10^{17}$) cm-3 for the N II, and Cd II spectral lines respectively.

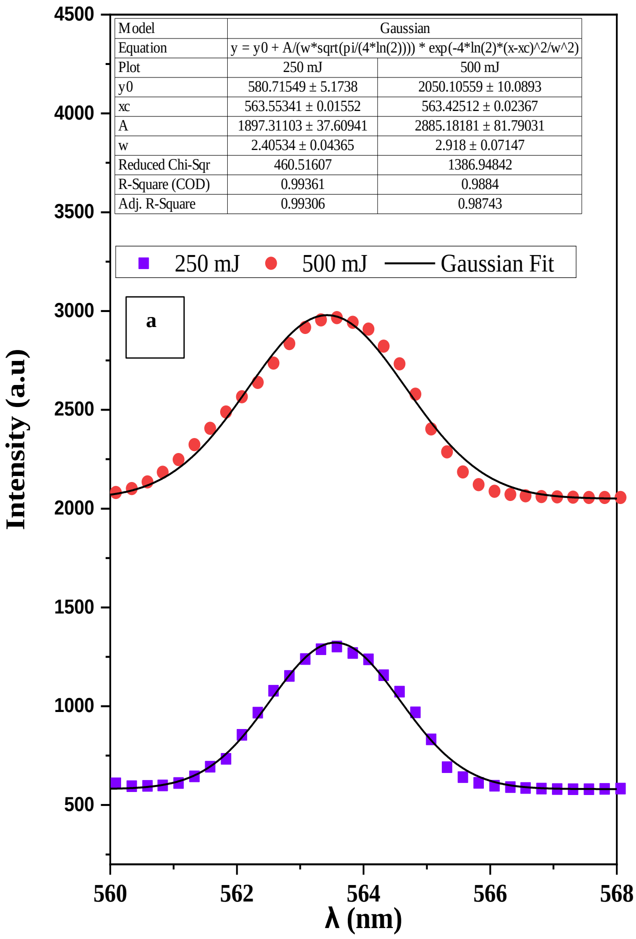


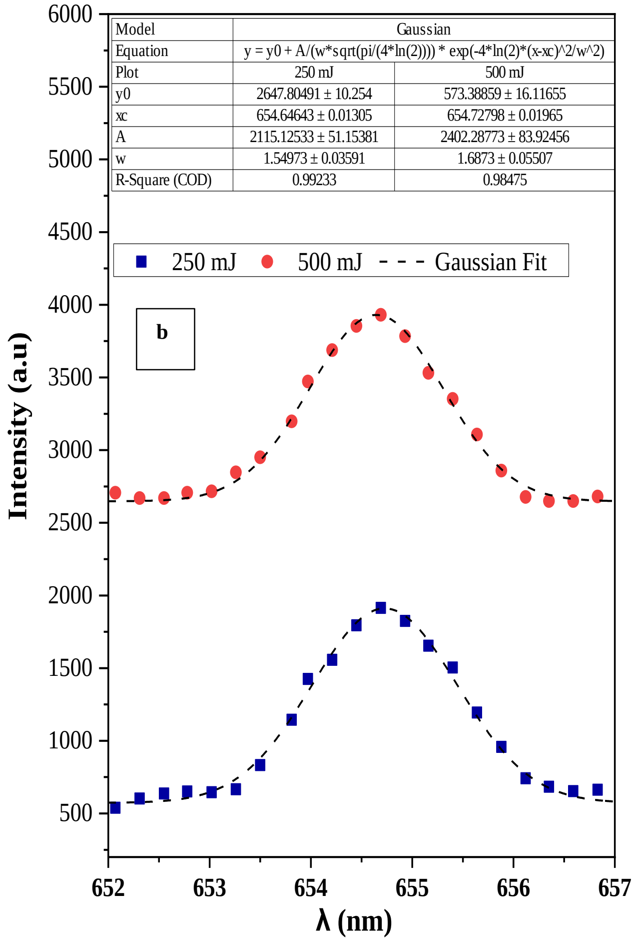


**Figure 6. Gaussian fitting of the (a) N (II) for FHG, and (b) (Cd II) for SHG transition for a variety of energies.**

The research findings demonstrate a direct correlation between the laser's intensity and the electron density of the plasma. Increasing the intensity of a laser leads to heightened interactions with the material it is composed of, resulting in an elevated level of ionization and electron production. Consequently, an augmentation in the laser power frequently leads to an elevation in the electron density within the plasma.

The intensity of the line at 532 nm is lower compared to that of the 1064 nm laser. The laser exhibits a reduction in the number of photons by half, while simultaneously doubling the energy per photon. Furthermore, the exit energy can be reduced by going through the second harmonic crystal [28].

In contrast, the plasma density exhibited a decrease, although the plasma temperature demonstrated an

Published Online First: June, 2024
https://doi.org/10.21123/bsj.2024.9322
P-ISSN: 2078-8665 - E-ISSN: 2411-7986
Baghdad Science Journal

increase when employing a laser with a second harmonic wavelength (532 nm) in comparison to the fundamental wavelength (1064 nm) as shown in Fig. 7. This can be attributed to the reduction in the number of photons possessing twice the energy of the photons, resulting in a halving effect. Hence, the ionization phenomenon occurs in a reduced number of atoms, resulting in a decreased production of electrons. However, these electrons exhibit greater thermal velocity when subjected to the laser-material interaction inside the field emission mechanism [29].

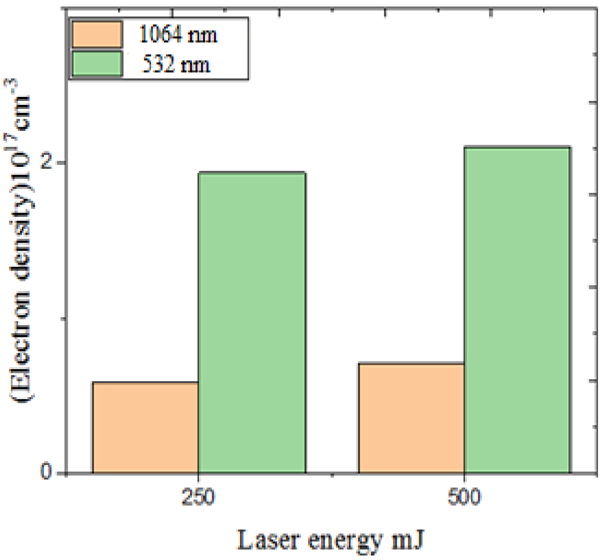


**Figure 7. The electron density at λ 1064 and 532 nm as a function of laser energy**

**Debye Length $\lambda_d$, Plasma Frequency $f_p$**

After determining the Te in eV and $n_e$ in $^1/_{cm^3}$, it is now able to compute the $\lambda_d$ in cm using equation [30]:

$$\lambda_d = \sqrt{\frac{\varepsilon_O K_B T_e}{e^2 n_e}} \dots\dots\dots 4$$

If we express the preceding equation as [30], where $\varepsilon_O$represents the permittivity of the vacuum, $K_B$ stands for the Boltzmann constant, and e stands for the charge of an electron, then we have:

$$\lambda_d = 7430\left(\frac{T}{n_e}\right)^{\frac{1}{2}} (cm) \dots\dots\dots 5$$

The frequency of plasmas may be described as follows [4]:

$$f_p = \frac{n_e e^2}{m_e \varepsilon_\circ} \dots\dots\dots 6$$

Where is the $f_p$The frequency of the plasmas is an extremely important aspect, and the electron mass is denoted by $m_e$

To get the Debye number, another option is to apply the following equation:

$$N_D = \frac{4}{3}\pi n_e \boldsymbol{\lambda}_D^3 = 1.38 \times 10^6 T^{3/2} n_e^{1/2} \dots\dots\dots 7$$

The pulse's intensity causes the plasma's electrons to heat up. This is consistent with previous research for Cd and other elements that showed raising the strength of pulses raised both $T_e$ and $n_e$ in the Cadumuim plasmas. Tables 3, and 4 numbers back up this claim. We note that as the laser pulse energy increases, the Debye length (λD) decreases; This is because lasers can have different effects on plasma, depending on their intensity and frequency. However, in general, increasing the energy of the laser pulse increases the temperature (Te) of the material by an amount sufficient to separate the outermost electron from the atom, and thus leads to a significant increase in electron density.

**Table 3. Plasma Parameters from Cd plasma plume by first harmonic generation laser (FHGL)**

| λ = 1064 nm | | | | | | | | |
|---|---|---|---|---|---|---|---|---|
| **E (mJ)** | **$T_e$ (eV)** | **FWHM (nm)** | **$\omega_s$ (nm)** | **$N_r \times 10^{17}$ ($cm^{-3}$)** | **$N_e \times 10^{16}$ ($cm^{-3}$)** | **$\lambda_D \times 10^{-6}$ (cm)** | **$f_P \times 10^{12}$ (Hz)** | **$N_D \times 10^2$ particle** |
| 250 | 1.063 | 2.41 | 2.04 | 0.99 | 5.84 | 3.17 | 2.17 | 7.79 |
| 500 | 1.299 | 2.92 | 2.04 | 0.99 | 7.08 | 3.18 | 2.39 | 9.56 |

Published Online First: June, 2024
https://doi.org/10.21123/bsj.2024.9322
P-ISSN: 2078-8665 - E-ISSN: 2411-7986
Baghdad Science Journal

**Table 4. Plasma Parameters from Cd plasma plume by second harmonic generation laser (SHGL)**

| λ = 532 nm | | | | | | | | |
|---|---|---|---|---|---|---|---|---|
| **E (mJ)** | **$T_e$ (eV)** | **FWHM (nm)** | **$\omega_s$ (nm)** | **$N_r \times 10^{17}$ ($cm^{-3}$)** | **$N_e \times 10^{17}$ ($cm^{-3}$)** | **$\lambda_D \times 10^{-6}$ (cm)** | **$f_P \times 10^{12}$ (Hz)** | **$N_D \times 10^2$ particle** |
| 250 | 0.74 | 1.55 | 0.400 | 1.00 | 1.94 | 1.45 | 3.95 | 2.47 |
| 500 | 0.82 | 1.69 | 0.400 | 1.00 | 2.11 | 1.46 | 4.12 | 2.75 |

The increase in electron temperature found when using a primary laser with a longer wavelength compared to a second harmonic laser can be attributed to several factors, such as differences in laser-plasma interactions, energy absorption, or heating mechanisms. To determine the exact cause, a thorough investigation of the experimental setup, the interactions between the laser and plasma, and the underlying physics mechanisms would be necessary. It is postulated that the interaction between the plasma and the laser with longer wavelengths may result in an augmented transfer of energy to the electrons. The potential correlation between the rise in electron temperature and the utilization of a primary laser with a longer wavelength could be attributed to variances in energy deposition and absorption mechanisms. Wavelengths of greater length possess the ability to penetrate the plasma to a greater extent, so engaging with a larger quantity of particles facilitates the transfer of a greater amount of energy to the electrons. The increased energy absorption observed in this scenario may result in elevated electron temperatures in comparison to the second harmonic laser with a lower wavelength, which may exhibit limited penetration into the plasma.

## Conclusion

Overall, this study compared laser-induced plasma from the primary and secondary harmonic frequencies of a cadmium metal target and examined plasma plume morphology, elemental composition, and spectrum emissions. This study revealed subtle differences between the two harmonic wavelengths' characteristics and behaviors through careful experimentation and data analysis. These findings affect spectroscopy, material science, and laser applications. As scientists study laser-plasma interactions, adding variables may provide even more deep findings. The effect of laser parameters (i.e., energy and wavelength) on the Cadmium plasma plume heating was studied. Plasma temperatures are the highest in the fundamental laser (1064 nm) case compared with the second harmonic (532 nm) case; The electron density in the plasma plume at λ (532) nm is slightly higher than at λ (1064) nm; These results can be explained in shorter wavelengths by the effect of an increased mass ablation rate because Shorter wavelengths correspond to higher energy photons. When these photons interact with the material, they impart more energy per photon, which can lead to increased bond-breaking and material removal.

## Acknowledgment

We thank the Medical Physics Lab., Department of Physics, College of Science for Women, University of Baghdad.

## Authors' Declaration

- Conflicts of Interest: None.
- We hereby confirm that all the Figures in the manuscript are ours. Furthermore, any Figures and images, that are not ours, have been included with the necessary permission for re-publication, which is attached to the manuscript.
- No animal studies are present in the manuscript.
- No human studies are present in the manuscript.

Published Online First: June, 2024
https://doi.org/10.21123/bsj.2024.9322
P-ISSN: 2078-8665 - E-ISSN: 2411-7986
Baghdad Science Journal

- Ethical Clearance: The project was approved by the local ethical committee at University of Baghdad.

## Authors' Contribution Statement

N. Kh. A, T. A. Kh. contributed to the design and implementation of the research, the analysis of the results, and the writing of the manuscript.

## References

1. Hanif M, Salik M, Arif F. Spectroscopic Study of Carbon Plasma Produced by the First (1064 nm) and Second (532 nm) Harmonics of Nd : YAG Laser. Plasma Phys Reports. 2015; 41(3): 274–80. https://dx.doi.org/10.1134/S1063780X15030034
2. Chiang WH, Mariotti D, Sankaran RM, Eden JG, Ostrikov K. Microplasmas for Advanced Materials and Devices. Adv Mater. 2020; 32(18). https://doi.org/10.1002/adma.201905508
3. Murtaza G, Shaikh NM, Kandhro GA, Ashraf M. Laser-induced breakdown optical emission spectroscopic study of silicon plasma. Spectrochim Acta - Part A Mol Biomol Spectrosc [Internet]. 2019; 223: 117374. https://doi.org/10.1016/j.saa.2019.117374.
4. Mazhir SN, Abdullah NA, Al-Ahmed HI, Harb NH, Abdalameer NK. The effect of gas flow on plasma parameters induced by microwave. Baghdad Sci J. 2018; 15(2): 205-210. https://doi.org/10.21123/bsj.2018.15.2.0205.
5. Murbat HH, Abdalameer NKH, Brrd AK, Abdulameer F. Effects of non-thermal argon plasma produced at atmospheric pressure on the optical properties of CdO thin films. Baghdad Sci J. 2018; 15(2): 221–6. https://doi.org/10.21123/bsj.2018.15.2.0221.
6. Yao H, Asamoah E, Wei P, Cong J, Zhang L, Quaisie JK, et al. Investigation into the effect of increasing target temperature and the size of cavity confinements on laser-induced plasmas. Metals (Basel). 2020; 10(3): 2-15. doi: 10.3390/met10030393
7. Zaitun Prasetyo S, Suliyanti MM, Isnaeni Herbani Y. Quantitative analysis of titanium concentration using calibration-free laser-induced breakdown spectroscopy (LIBS). J Phys Conf Ser. 2018; 985(1): 0–5. https://doi.org/10.1088/1742-6596/985/1/012010
8. Abbas NK, Abdulameer AF, Ali RM, Alwash SM. The Effect of Heat Treatment on Optical Properties of Copper (II) Phthalocyanine Tetrasulfonic Acid Tetrasodium Salt (CuPcTs) Organic Thin Films. Silicon . 08 april 2019; 11(2): 843–55.
9. N. K. Abdalameer, N. A. Yasoob, och A. Q. Mohammed, "Detection of Silica in Rice Husks Using Laser-Induced Plasma and Studying the Effect of Laser Energy on the Parameters of the Produced Plasma", Int. J. Nanosci., vol. 23, nr 3, s. 1–9, 2024, doi: 10.1142/S0219581X23500783
10. Ismail M a., Imam H, Elhassan A, Youniss WT, Harith M a. LIBS limit of detection and plasma parameters of some elements in two different metallic matrices. J Anal At Spectrom. 2004; 19(4): 489.
11. Hussain T, Gondal MA. Laser induced breakdown spectroscopy (LIBS) as a rapid tool for material analysis. J Phys Conf Ser. 10 juni 2013; 439(1): 012050.
12. Mazalan E, Chaudhary K, Haider Z, Abd Hadi SF, Ali J. Determination of calcium to phosphate elemental ratio in natural hydroxypatite using LIBS. J Phys Conf Ser. 2018; 1027(1): 012013.
13. Ahmed BM. Plasma Parameters Generated from Iron Spectral Lines By Using LIBS Technique. IOP Conf Ser Mater Sci Eng. 01 november 2020; 928(7): 072096.
14. Murtaza G, Shaikh NM, Kandhro GA, Ashraf M. Laser induced breakdown optical emission spectroscopic study of silicon plasma. Spectrochim Acta Part A Mol Biomol Spectrosc. december 2019;223:117374. https://doi.org/10.1016/j.saa.2019.117374
15. Zaitun Prasetyo S, Suliyanti MM, Isnaeni Herbani Y. Quantitative analysis of titanium concentration using calibration-free laser-induced breakdown spectroscopy (LIBS). J Phys Conf Ser. 2018;985(1):012010.
16. National Institute of Standards and Technology (NIST) atomic spectra database (version 5), https://physics.nist.gov/PhysRefData/ASD/lines_form.html. (version 5).
17. Ruan F, Zhang T, Li H. Laser-induced breakdown spectroscopy in archeological science: a review of its application and future perspectives. Appl Spectrosc Rev. 2019; 54(7): 573–601. https://doi.org/10.1080/05704928.2018.1491857
18. Hanif M, Salik M, Baig MA. Diagnostic Study of Nickel Plasma Produced by Fundamental ( 1064 nm ) and Second Harmonics ( 532 nm ) of an Nd : YAG Laser. J Mod Phys. 2012; 3(30): 1663-1669.

https://doi.org/10.4236/jmp.2012.330203
19. Hanif M, Salik M, Baig MA. Quantitative studies of copper plasma using laser-induced breakdown spectroscopy. Opt Lasers Eng. 2011; 49(12): 1456–61. https://dx.doi.org/10.1016/j.optlaseng.2011.06.013
20. Anabitarte F, Cobo A. Laser-Induced Breakdown Spectroscopy : Fundamentals, Applications, and Challenges. International Scholarly Research Network. 2012; ID 285240, P12. https://doi.org/10.5402/2012/285240.
21. Sullivan GO, Li B, Arcy RD, Wu T, Wang X, Lu H. Laser wavelength dependence on angular emission dynamics of Nd : YAG laser-produced Sn plasmas. Plasma Sources Sci. Technol. 2012; 21:7. https://doi.org/10.1088/0963-0252/21/5/055003
22. Torrisi L, Caridi F, Giuffrida L. Comparison of Pd plasmas produced at 532 nm and 1064 nm by a Nd : YAG laser ablation. Nucl Inst Methods Phys Res B. 2010; 268(13): 2285–91. http://dx.doi.org/10.1016/j.nimb.2010.03.029
23. Haq SU, Ahmat L, Mumtaz M, Shakeel H, Mahmood S, Nadeem A. Spectroscopic studies of magnesium plasma produced by fundamental and second harmonics of Nd : YAG laser Spectroscopic studies of magnesium plasma produced by fundamental and second harmonics of Nd : YAG laser. Phys Plasmas. 2015; 22(083504): 1–8. http://dx.doi.org/10.1063/1.4928376
24. Abbas Q. A. Effect of target properties on the plasma characteristics that produced by laser at atmospheric pressure. Iraqi J. Sci. 60(6):1251-8. 2019. https://doi.org/10.24996/ijs.2019.60.6.8.
25. Mazalan E, Chaudhary K, Haider Z, Abd Hadi SF, Ali J. Determination of calcium to phosphate elemental ratio in natural hydroxyapatite using LIBS. J Phys Conf Ser. 2018; 1027(1): 1–8. doi: 10.1088/1742-6596/1027/1/012013
26. Hussain Shah SK, Iqbal J, Ahmad P, Khandaker MU, Haq S, Naeem M. Laser induced breakdown spectroscopy methods and applications: A comprehensive review. Radiat. Phys. 2020 May;170:108666. https://doi.org/10.1016/j.radphyschem.2019.10866.
27. Asamoah E, Xia Y, Hongbing Y, Wei P, Jiawei C. Influence of cavity and magnetic confinements on the signal enhancement and plasma parameters of laser-induced Mg and Ti plasmas. Laser Part Beams. 2020; 38(1): 1–12. https://doi.org/10.1017/S0263034620000014
28. Ruthandi M, Okamoto Y, Hamada K, Okada A, Nakashima S, Nishi N. Effects of superposition of 532 nm and 1064 nm wavelengths in copper micro-welding by pulsed Nd : YAG laser. J Mater Process Technol. 2022; 299: 11-13. https://doi.org/10.1016/j.jmatprotec.2021.117388
29. Ã NG, Elliott G. The effect of ambient pressure on laser-induced plasmas in air. Opt Lasers Eng. 2007; 45: 27–35. https://doi.org/10.1016/j.optlaseng.2006.04.002
30. Farka Z, Vytisková K, Makhneva E, Zikmundová E, Holub D, Buday J, et al. Comparison of single and double pulse laser-induced breakdown spectroscopy for the detection of biomolecules tagged with photon-upconversion nanoparticles. Anal. Chim. Acta. 2024 Apr 1;1299:342418–8. https://doi.org/10.1016/j.aca.2024.342418.

Published Online First: June, 2024
https://doi.org/10.21123/bsj.2024.9322
P-ISSN: 2078-8665 - E-ISSN: 2411-7986

Baghdad Science Journal

# التحليل المقارن للبلازما المتولدة باستخدام تقنية LIBS لأطوال موجية مختلفة لليزر النبضي لهدف الكادميوم

**تقى اكرم خليفة، نسرين خليل عبد الامير**

قسم الفيزياء، كلية العلوم للبنات، جامعة بغداد، بغداد، العراق.

## الخلاصة

الهدف من هذه الدراسة هو تحليل الخواص الطيفية للبلازما المنتجة من الكادميوم (Cd) باستخدام طريقة التحليل الطيفي للانهيار المستحث بالليزر (LIBS). استخدمت عملية توليد البلازما الليزر التوافقي الأساسي (1064 نانومتر) والليزر التوافقي الثانوي (532 نانومتر) الثاني (SHL) لليزر المخدر بالنيوديميوم Q-switched. يستخدم عقيق الألومنيوم الإيتريوم (YAG) كمادة بلورية. تبلغ مدة نبضات الليزر 10 نانوثانية، ومعدل تكرار 8 هرتز، وكانت مخرجات الطاقة 250 (ملي جول) و500 (ملي جول) عند أطوال موجية 1064 (نانومتر) و532 (نانومتر)، على التوالي. تم تحقيق التركيز الدقيق للشعاع من خلال تركيز الليزر على المادة المستهدفة، والتي تتكون من 100% من الكادميوم. تم قياس درجة حرارة الإلكترون باستخدام طريقة مؤامرة بولتزمان من خلال تسخير البيانات التجريبية للخصائص الخطية المرتبطة بالخطوط المحايدة (Cd II)، (O II)، (N II)، وخطوط الأيونات (Cd I)، (O I) لمدة (1064 ، 532 نانومتر. أدى استخدام المنهجية التحليلية إلى تحديد قيم درجة حرارة الإلكترون من 8584 كلفن إلى 15068.4 كلفن للتوافقيات الأساسية والثانية لليزر على التوالي. في الوقت نفسه، تم تحديد كثافة الإلكترون (ne) من خلال تحليل ملف تعريف توسيع ستارك المرتبط بخط الكادميوم المحايد. يتم تحديد خصائص البلازما (درجة حرارة الإلكترون وكثافة الإلكترون) عن طريق تعديل طاقة الليزر على سطح الهدف، طوليًا على طول مسار عمود البلازما.

**الكلمات المفتاحية:** درجة حرارة الالكترون، توسيع ستارك، طريقة مخطط بولتزمان، مطياف الانهيار المستحث بالليزر، كثافة الالكترون، الليزر التوافقي الثاني.